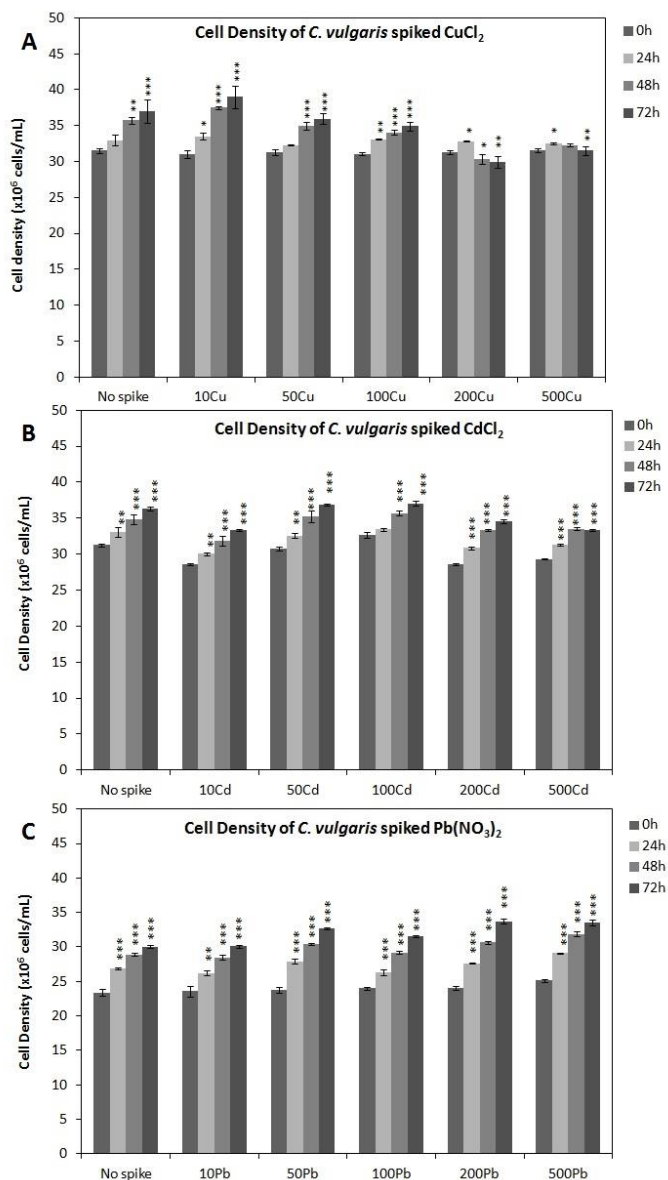


## Supporting document

Supplementary Figure S1 showed the cell density of *Chlorella vulgaris* exposed to different concentrations of  $\text{CuCl}_2$ ,  $\text{CdCl}_2$  and  $\text{Pb}(\text{NO}_3)_2$ , recorded at 0h, 24h, 48h and 72 hours respectively using UV spectrometer ( $\text{OD}_{442.5}$ )



**Figure S1.** Cell density of *C. vulgaris* spiked with different metal treatments. Cultures ( $3 \times 10^7$  cells/mL) exposed to 0, 10, 50, 100, 200 and 500  $\mu\text{M}$  of (A)  $\text{CuCl}_2$ , (B)  $\text{CdCl}_2$ , (C)  $\text{Pb}(\text{NO}_3)_2$  for a period of 0h (■), 24h (■), 48h (■) and 72h (■). Significant  $p < 0.05$  (\*),  $p < 0.01$  (\*\*),  $p < 0.001$  (\*\*\*)

The comparison between principal component analysis (PCA) and orthogonal partial least square discriminant analysis (OPLS-DA) were displayed in Supplementary Figure S2.

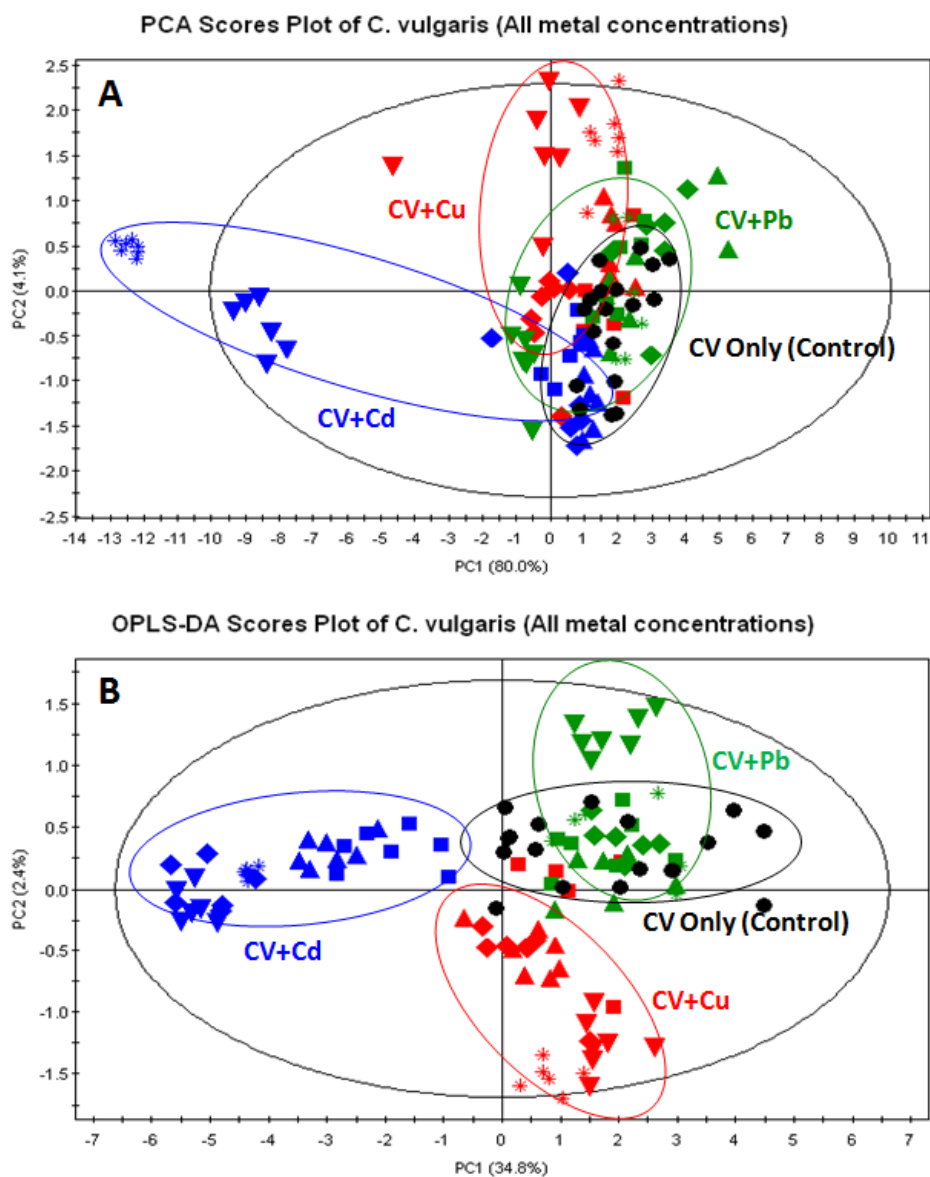
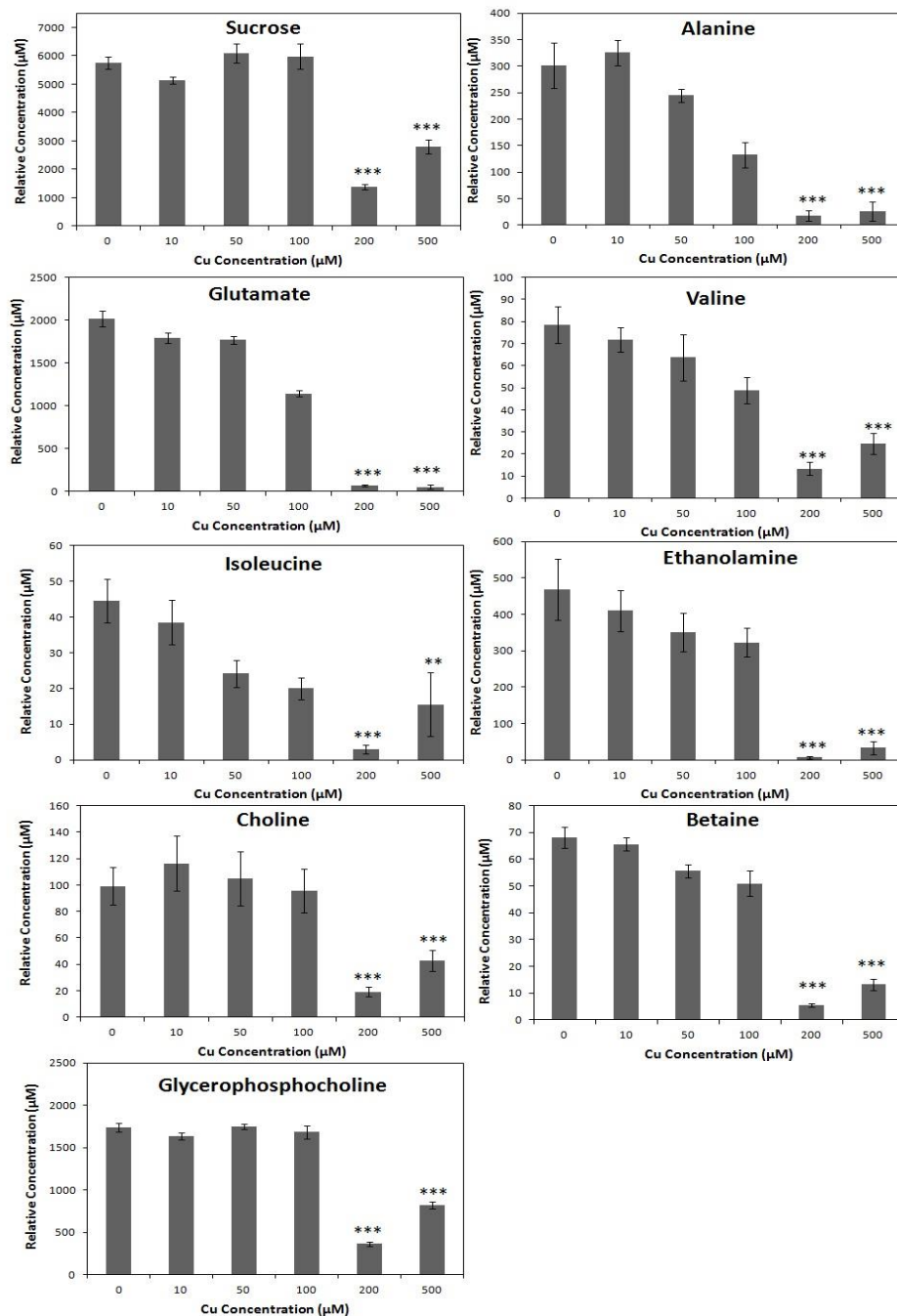


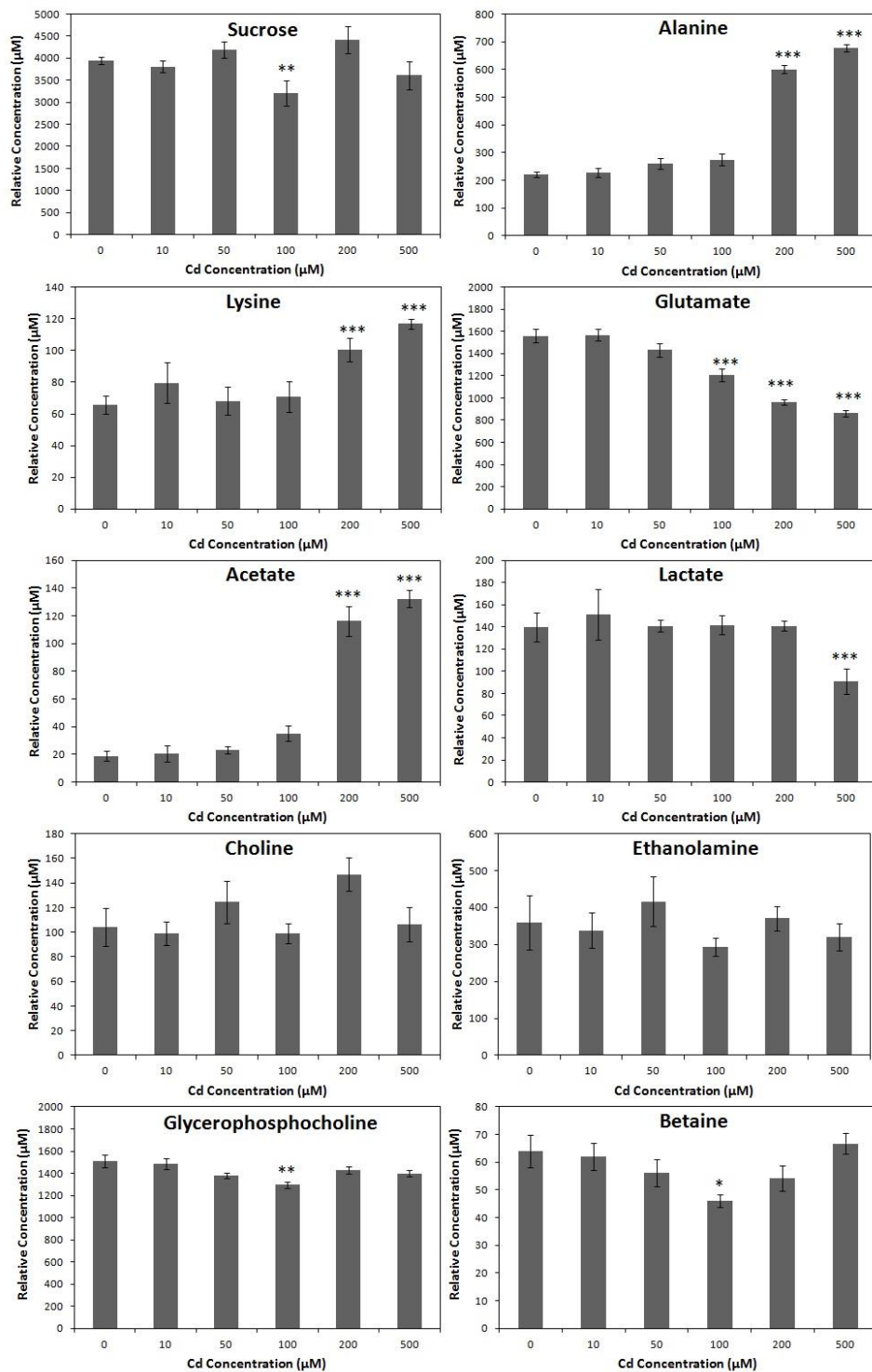
**Figure S2.** Multivariate analysis scatter scores plot for *C. vulgaris* control and cultures spiked with different metal solutions. (A) PCA, (B) OPLS-DA.

Metal concentration dependent changes of metabolites determined to have significantly influenced the differentiation observed in OPLS-DA scores plot (Figure 2) and OPLS-DA loadings plot (Figure 3). The column plot in Supplementary Figure S3 shows the changes in the relative concentration of various metabolites when the culture medium was spiked with different concentrations of a)  $\text{CuCl}_2$ , b)  $\text{CdCl}_2$ , c)  $\text{Pb}(\text{NO}_3)_2$

**A**



**B**



C

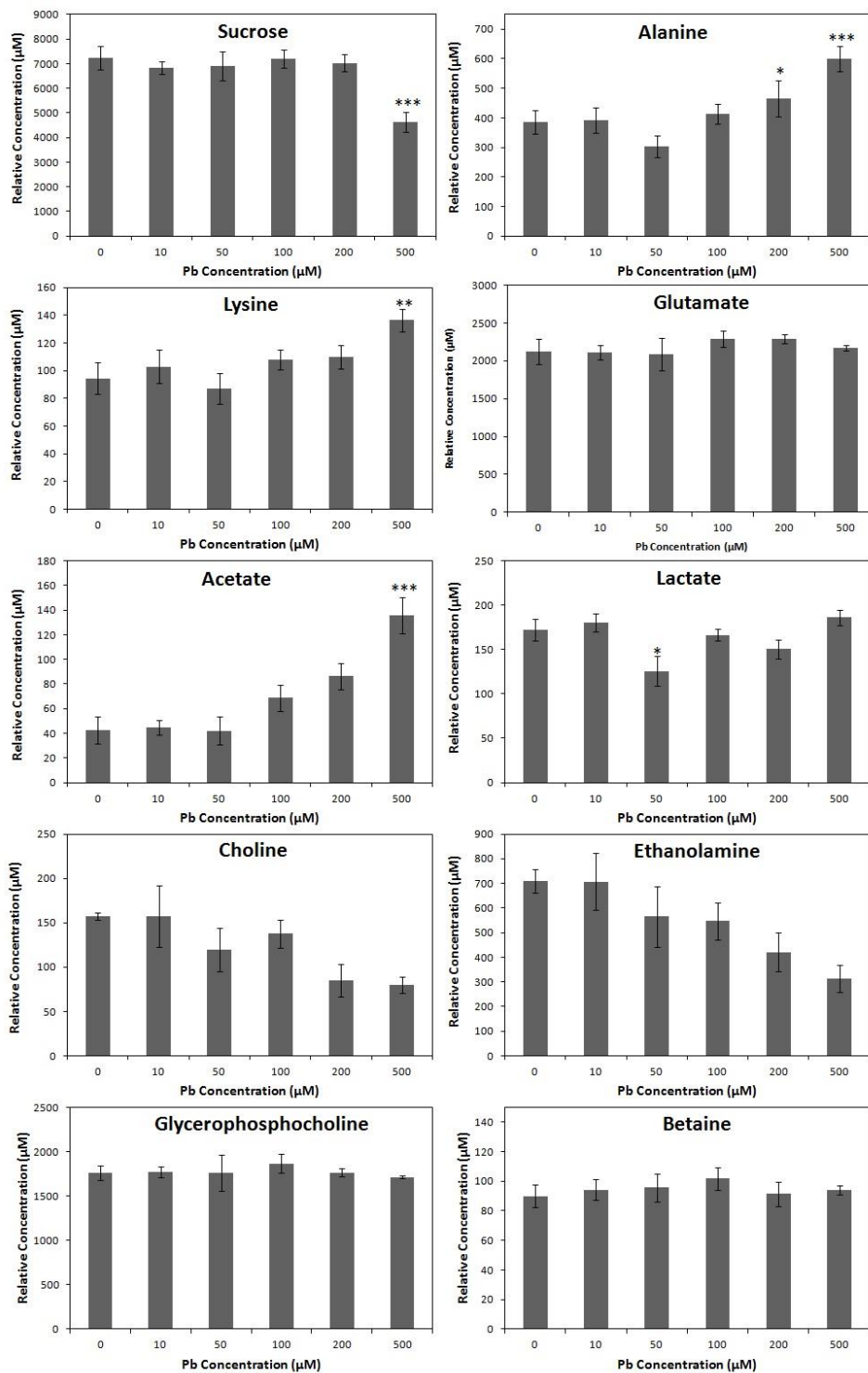
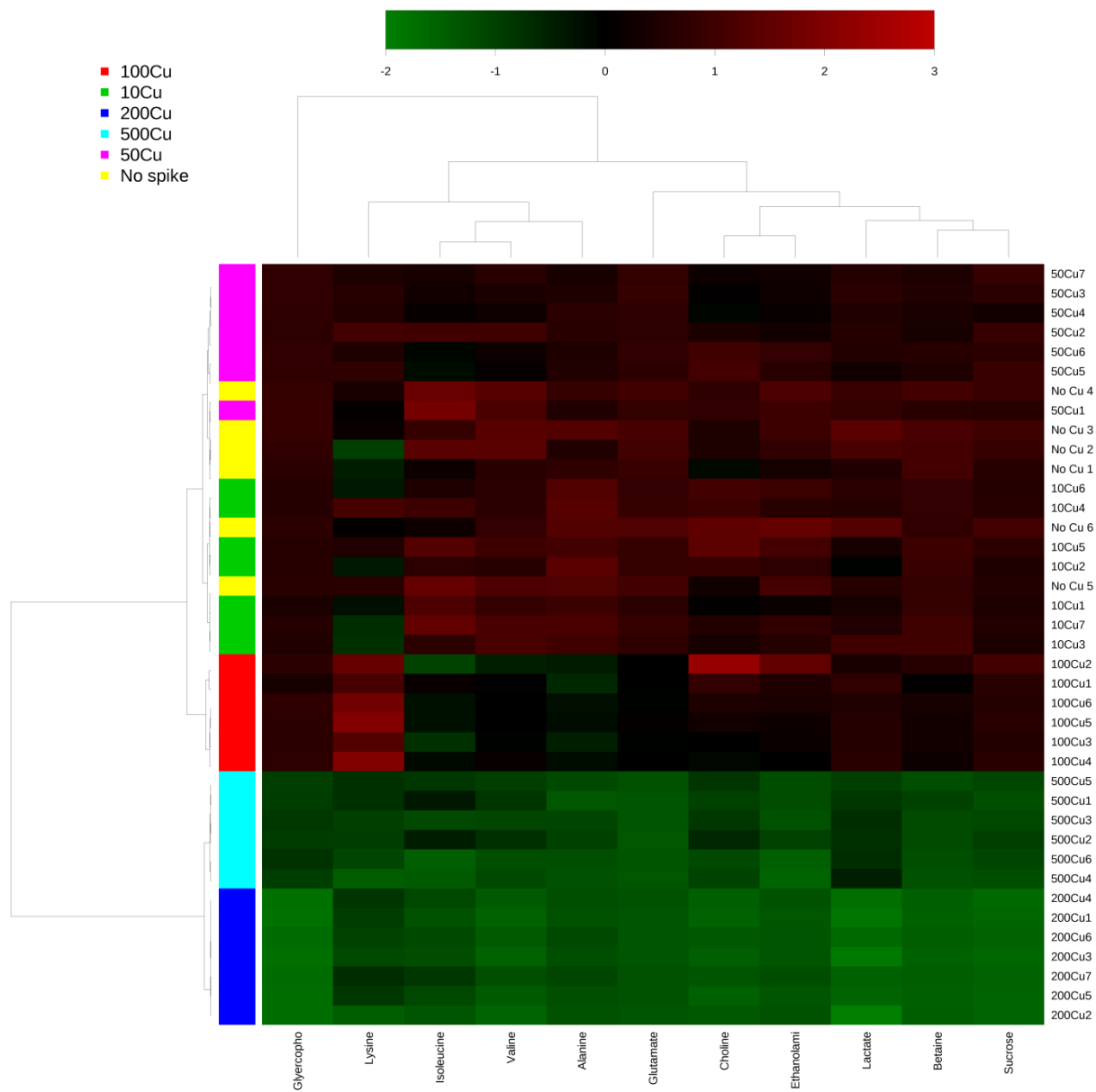
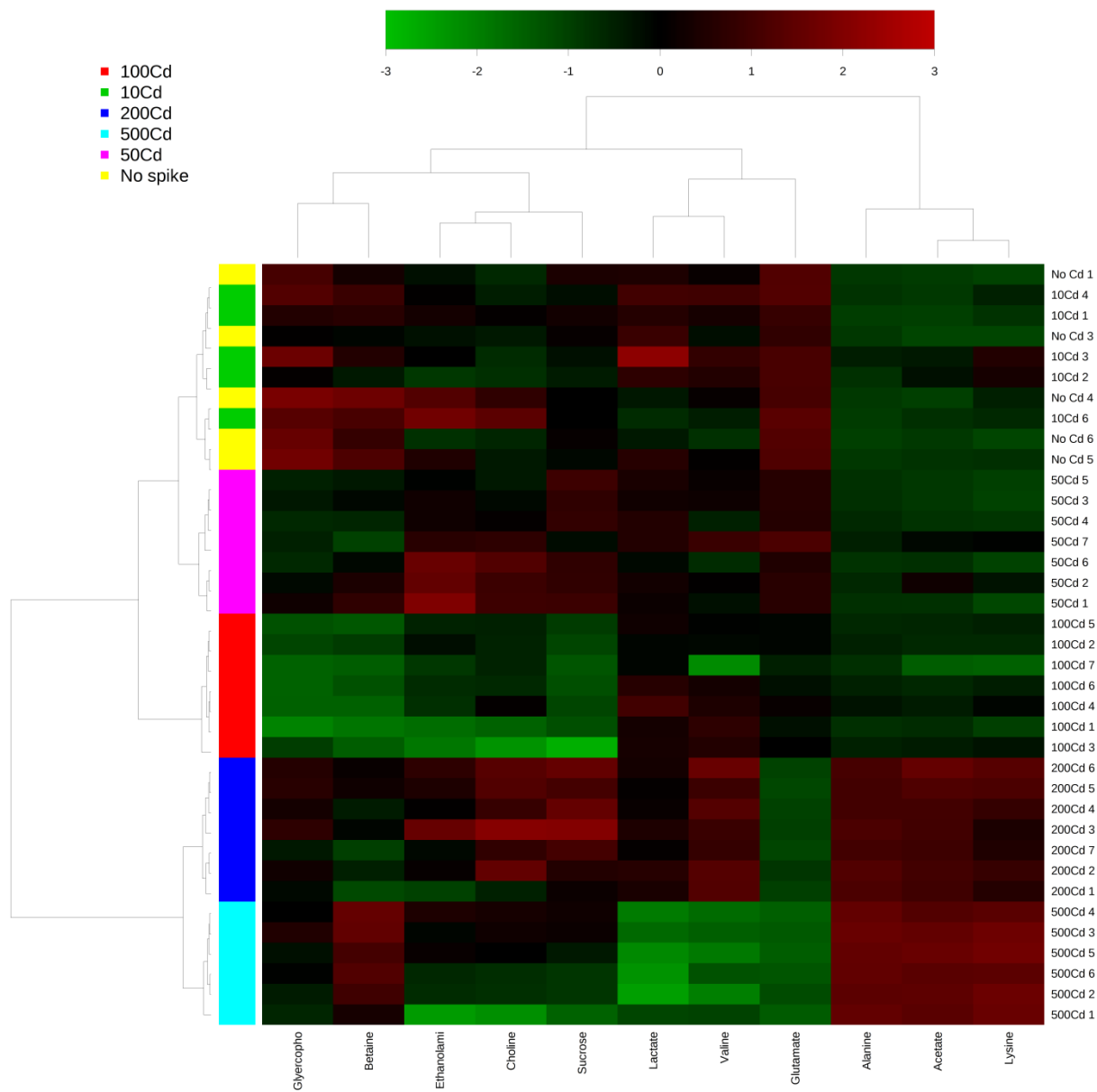


**Figure S3.** Effect of metal concentrations on *C. vulgaris* metabolome. Relative concentration of metabolites determined from NMR spectroscopy with reference to 0.5 mM DSS, when *C. vulgaris* was spiked with various concentrations (0, 10, 50, 100, 200 and 500  $\mu\text{M}$ ) of a)  $\text{CuCl}_2$ ; b)  $\text{CdCl}_2$ ; 3)  $\text{Pb}(\text{NO}_3)_2$ . Significantly level determined as \* ( $p < 0.05$ ), \*\* ( $p < 0.01$ ), \*\*\* ( $p < 0.001$ ).

A



**B**



C

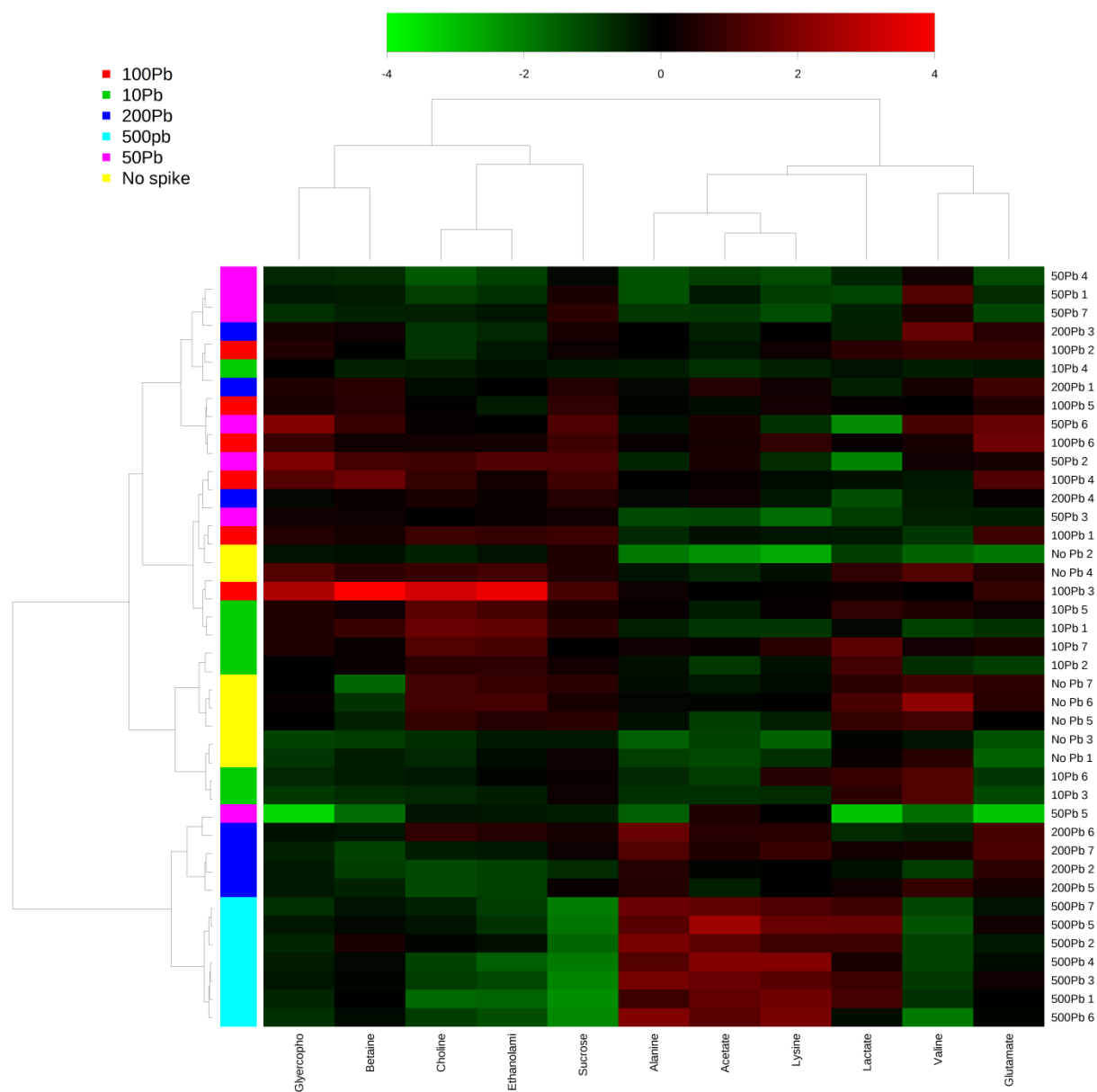
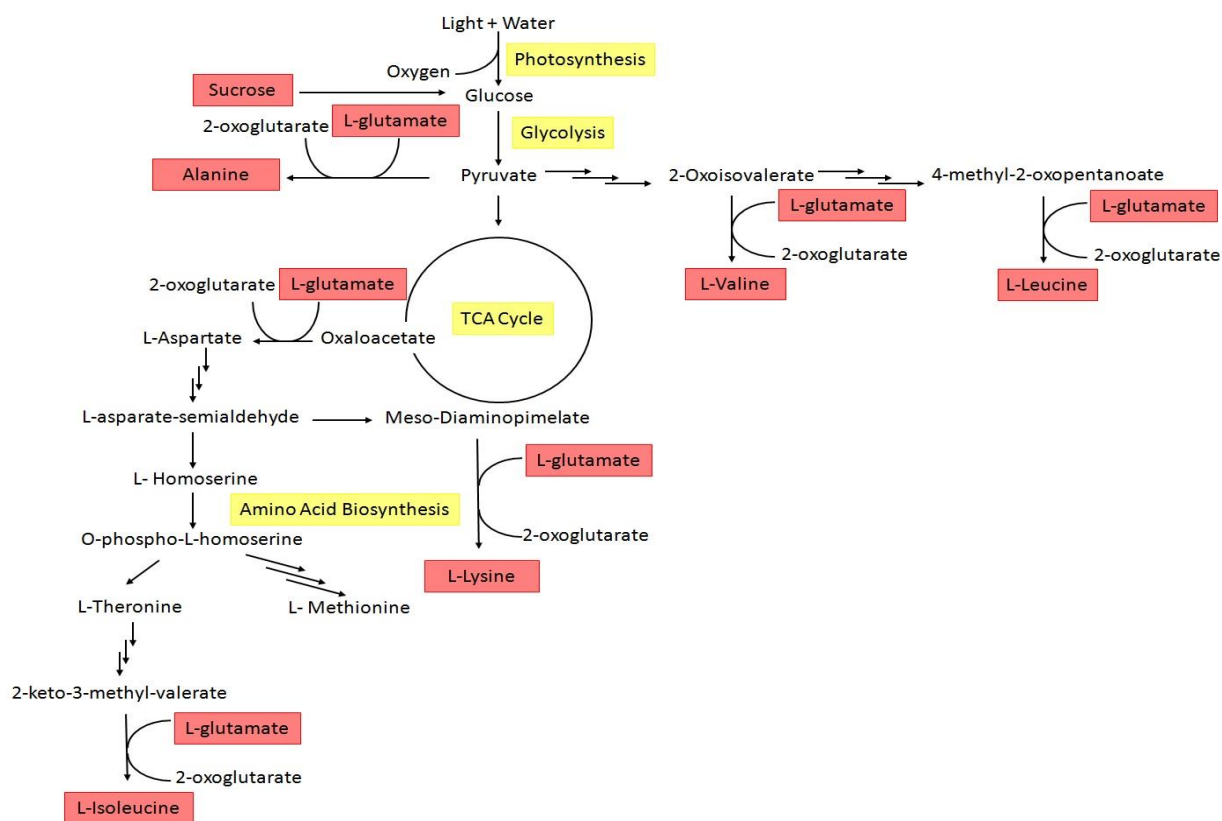


**Figure S4.** Heatmap correlation of *C. vulgaris* polar extract  $^1\text{H}$  NMR spectra. Correlation of metabolites responsible for (A) Cu-induced stress; (B) Cd-induced stress; (C) Pb-induced stress in *C. vulgaris*.

**A**



**B**

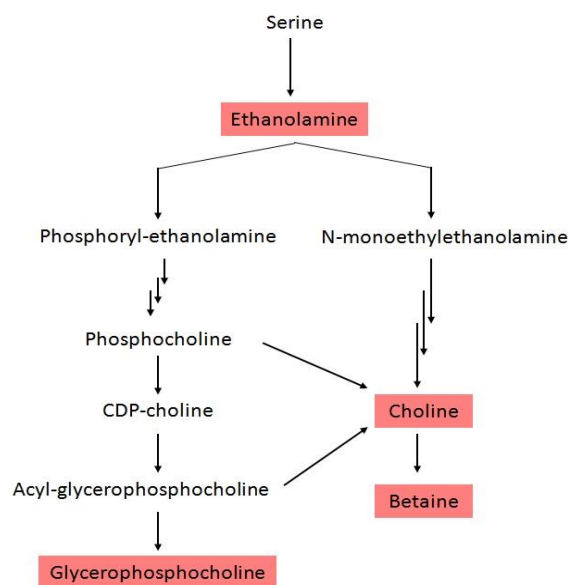


**Figure S5.** Copper induced metabolic changes in *C. vulgaris*. (A) Photosynthesis impairment arise from Cu-induced stress were demonstrated using the carbohydrate metabolism and amino acid biosynthesis pathways (yellow). (B) Cu-induced oxidative stress. Metabolites which were significantly ( $p < 0.001$ ) reduced were highlighted in red.

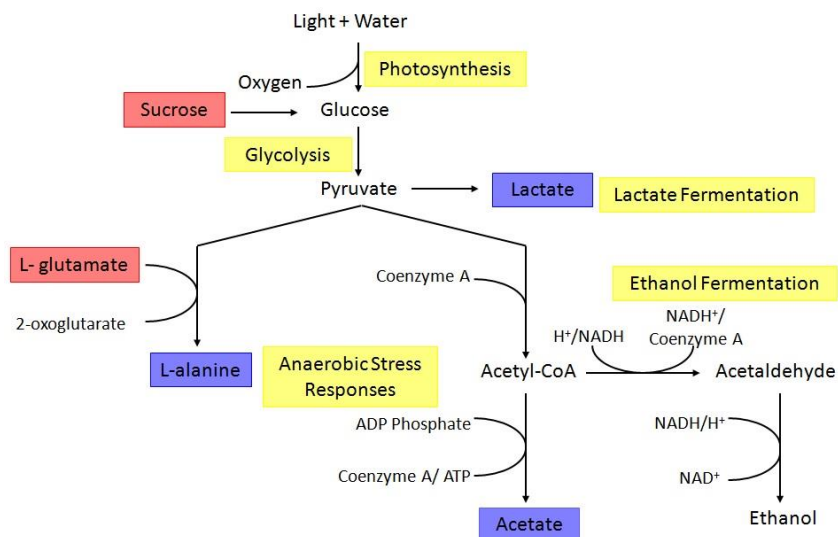


**Figure S6.** Cadmium and lead induced metabolic changes in *C. vulgaris*. Anaerobic stress responses arise from exposure to high Cd and Pb concentrations were demonstrated using anaerobic fermentation pathways (yellow). Metabolites which were significantly ( $p < 0.001$ ) increased were highlighted in blue, and reduced metabolites were shown in red.

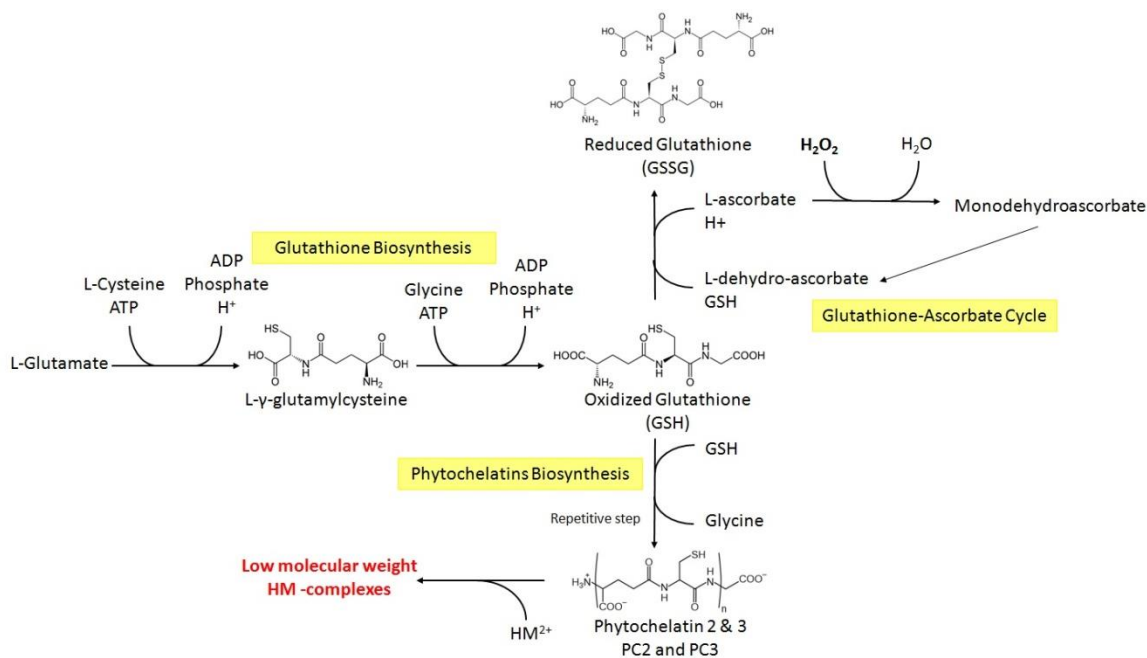


**Figure S7.** Proposed heavy metal (HM) detoxification mechanisms. High HM<sup>2+</sup> content in *C. vulgaris* cytoplasm induced the production of glutathione (GSH). To mediate metal toxicity in *C. vulgaris*, GSH act as both antioxidant and precursor of phytochelatin biosynthesis. Both metabolic pathways serve to reduce the availability of ROS and free HM<sup>2+</sup>, which would otherwise have adverse effects on the plant cells.